

# VFScale: Intrinsic Reasoning through Verifier-Free Test-time Scalable Diffusion Model

Tao Zhang\* Jia-Shu Pan\* Ruiqi Feng Tailin Wu\*<sup>†</sup>

Department of Artificial Intelligence, School of Engineering, Westlake University  
{zhangtao,panjiashu,fengruiqi,wutailin}@westlake.edu.cn

## Abstract

Inspired by human SYSTEM 2 thinking, LLMs excel at complex reasoning tasks via extended Chain-of-Thought. However, similar test-time scaling for diffusion models to tackle complex reasoning remains largely unexplored. From existing work, two primary challenges emerge in this setting: (i) the dependence on an external verifier indicating a notable gap from intrinsic reasoning of human intelligence without any external feedback, and (ii) the lack of an efficient search algorithm. In this paper, we introduce the Verifier-free Test-time Scalable Diffusion Model (VFScale) to achieve scalable intrinsic reasoning, which equips number-of-sample test-time scaling with the intrinsic energy function of diffusion models as the verifier. Concretely, VFScale comprises two key innovations to address the aforementioned challenges. On the training side, VFScale consists of a novel LRNCL loss and a KL regularization to improve the energy landscape, ensuring that the learned energy function itself serves as a reliable verifier. On the inference side, VFScale integrates the denoising process with a novel hybrid Monte Carlo Tree Search (hMCTS) to improve search efficiency. On challenging reasoning tasks of Maze and Sudoku, we demonstrate the effectiveness of VFScale’s training objective and scalable inference method. In particular, trained with Maze sizes of up to  $6 \times 6$ , our VFScale solves 88% of Maze problems with much larger sizes of  $15 \times 15$ , while standard diffusion model completely fails.

## 1 Introduction

Human intelligence can allocate more computation to solve harder problems, known as SYSTEM 2 thinking [1]. Motivated by this, large language models (LLMs) have exhibited promising performance in reasoning tasks through deliberate long Chain-of-Thought [2, 3]. Alongside LLMs, diffusion models have recently emerged as a compelling alternative. By casting reasoning as an optimization problem, these models iteratively refine candidate solutions toward higher-quality outputs. This approach has demonstrated strong potential, achieving notable results on tasks such as Sudoku solving, graph connectivity, and shortest-path computation [4, 5].

Although the iterative denoising procedure of diffusion models mirrors the repeated reasoning cycles required by complex reasoning tasks, their performance declines sharply once the problem difficulty exceeds the training distribution [4]. Moreover, prior works show that simply increasing the number of sampling steps quickly leads to a performance plateau [5]. Instead, in image generation, inference-time scaling to improve performance by increasing the number of samples has proven effective [6]. However, this strategy depends on an external verifier that is often unavailable or

\*Equal contribution.

<sup>†</sup>Corresponding author.

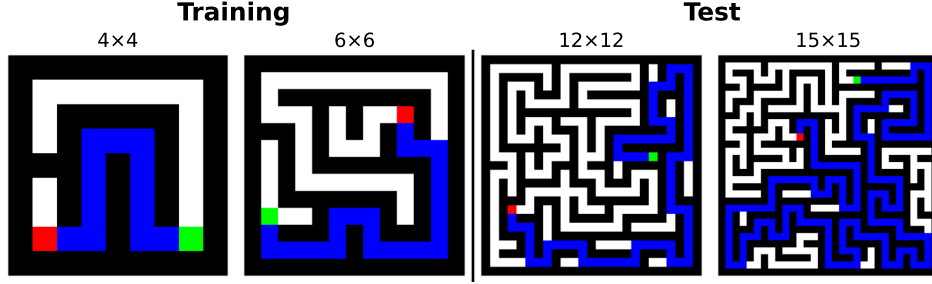


Figure 1: Visualizations of Maze training data and solutions generated by hMCTS denoising of our VFScale framework.

prohibitively expensive [7, 8]. Yet human intelligence can engage in deep, reflective intrinsic reasoning without any external feedback, revealing a clear gap with such methods [9, 10, 11]. These observations motivate our central question: *Can we design a Verifier-free Test-time Scalable Diffusion Model to achieve scalable intrinsic reasoning?*

In pursuit of such a test-time scalable intrinsic reasoning model, we leverage the fundamental mechanics of diffusion models. Diffusion models approximate the score function [12], which is equivalent to the negative gradient of the energy function. Our key insight is that the energy function, as a measure of the learned probability, can serve as an effective verifier itself. Based on the above premise, in this work, we explore equipping **number-of-sample test-time scaling** with diffusion models’ **intrinsic energy function**.

However, this strategy presents two primary challenges: **(1)** Firstly, using number-of-sample test-time scaling requires a verifier to evaluate and select samples. Prior work on test-time scaling has also established that verifier accuracy is crucial for performance [13, 6]. Consequently, using the energy function as an intrinsic verifier requires it to reliably reflect the sample quality. Nevertheless, previous energy-based diffusion models have largely ignored this requirement. **(2)** Secondly, the efficiency of the search algorithm is critical when scaling by varying the number of samples [14]. Nevertheless, the search efficiency of existing methods, such as best-of- $N$  (BoN), warrants further enhancement.

To approach these challenges, we propose Verifier-Free Test-Time Scalable Diffusion Models (VF-Scale), a novel framework designed to solve complex reasoning problems. VFScale consists of innovations in both training objectives and inference scaling as shown in Fig. 2 to respectively address the two aforementioned challenges. **(1)** On the training side, VFScale incorporates a novel Linear-Regression Negative Contrastive Learning (LRNCL) objective and a KL regularization to improve the energy landscape, especially to better align the energy function with sample quality with LRNCL loss. The LRNCL objective samples two negatives<sup>3</sup> for each positive sample and fits a linear regression between their energy values and their L2 distances to the positive. It encourages a positively sloped linear relationship, aligning the energy landscape with distance to the ground truth. We refer to this alignment as *performance-energy consistency*.<sup>4</sup> The KL regularization term backpropagates through the denoising process, smoothing the energy landscape. **(2)** On the inference side, we integrate the denoising process with a novel hybrid Monte Carlo Tree Search (hMCTS). It sequentially performs BoN and MCTS as the denoising proceeds. In the initial steps, BoN carries out parallel denoising without selecting to avoid premature exclusion of potential solutions, while the later MCTS denoising allows better navigation in the search space. Taken together, the hybrid MCTS denoising allows the model to significantly improve inference performance by scaling up the inference computational budget.

We demonstrate the effectiveness of our VFScale’s training objective and scalable inference method on challenging reasoning tasks of Maze and Sudoku. In Sudoku tasks, our VFScale solves 43% problems when conditioned on much less given digits (out-of-distribution condition), while the standard diffusion model only solves 30% problems. In Maze tasks, trained with Maze sizes of up to  $6 \times 6$ , VFScale successfully solves 88% of substantially larger  $15 \times 15$  instances (see Fig. 1), whereas the standard diffusion model fails entirely.

<sup>3</sup>Here, positive samples refer to data points, while negative samples correspond to noise-perturbed versions of the data.

<sup>4</sup>Detailed description for *performance-energy consistency* can be found in Appendix A.

In summary, our contributions are as follows: **(1)** We introduce Verifier-free Test-time Scalable Diffusion Models (VFScale), a novel framework that can scale up test-time computation for better reasoning capability. **(2)** We introduce Linear-Regression Negative Contrastive Learning (LRNCL) and KL regularization into the training objective to improve the energy landscape. **(3)** We integrate a hybrid Monte Carlo Tree Search into the denoising process, enabling test-time scaling with better search efficiency. **(4)** We demonstrate the effectiveness of our method on challenging Sudoku and Maze datasets where the conditions are out-of-distribution or the problem sizes are much larger.

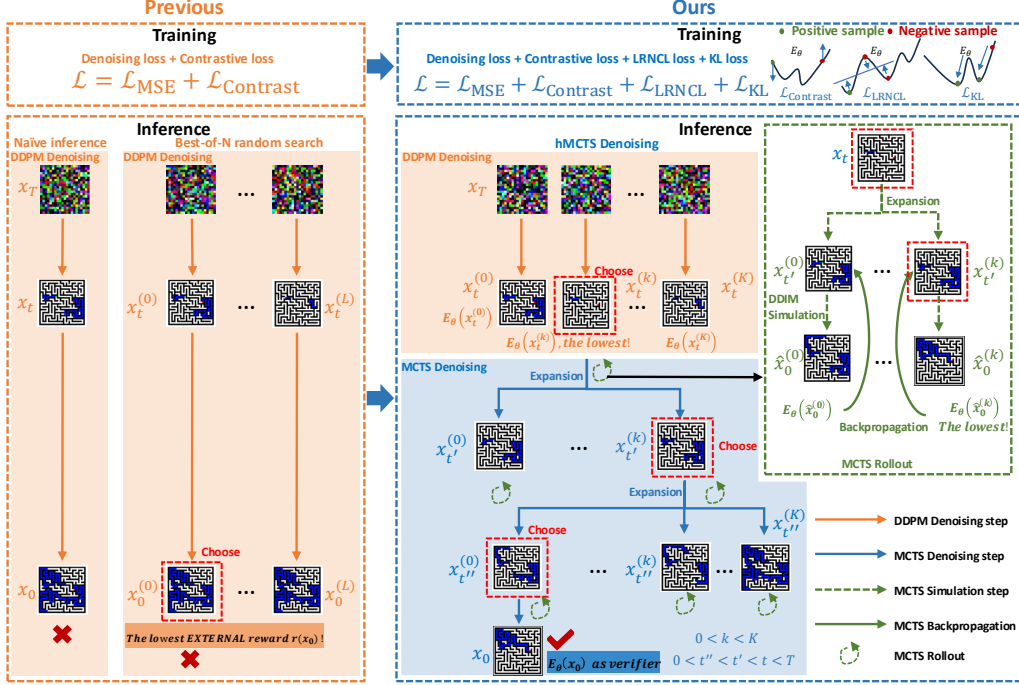


Figure 2: Overview of VFScale. This figure illustrates the key aspects of VFScale by contrasting its training and inference strategies with those of the previous method. **(1)** To qualify the intrinsic energy of diffusion models as a verifier, VFScale introduces  $\mathcal{L}_{\text{LRNCL}}$  and  $\mathcal{L}_{\text{KL}}$  to improve the energy landscape during training. **(2)** In order for a higher search efficiency, VFScale proposes hybrid Monte Carlo Tree Search (hMCTS) that achieves a balance between best-of- $N$  and MCTS.

## 2 Related Work

**Diffusion for Reasoning:** The iterative refinement process inherent in diffusion models lends itself well to tasks requiring multi-step reasoning. [4] firstly formulated multi-step reasoning as an energy minimization problem. To approach harder problems with more complex energy landscapes, more compute budget is used for optimization steps. [5] formulated the energy-based model as a diffusion model, and the performance on harder tasks was significantly improved. While effective, the performance gain by scaling the compute of these methods quickly saturates as the number of sampling steps increases. Building upon [5], VFScale instead explores number-of-sample scaling and proposes corresponding training and inference strategies.

**Test-time Scaling of Diffusion:** Improving diffusion model samples by increasing compute resources at inference time has emerged as an increasingly important direction. Early approaches focused on increasing the number of sampling steps, which leads to diminishing returns [15, 16]. More recent work [6, 17] has explored alternative scaling dimensions, such as increasing the number of sampled candidates, though these methods typically rely on external verifiers to guide solution selection. VFScale advances beyond these methods by leveraging the intrinsic energy function to guide test-time search, a capability further cultivated through customized training and inference strategies. These innovations make VFScale a versatile and scalable solution for real-world reasoning tasks.

### 3 Preliminary

The Denoising Diffusion Probabilistic Model (DDPM) [15] contains a predefined forward process to corrupt data into Gaussian noises, and a learnable reverse process to generate new samples from them. The forward process follows a Gaussian transition kernel  $q(\mathbf{x}_t|\mathbf{x}_{t-1}) = \mathcal{N}(\mathbf{x}_t|\sqrt{\alpha_t}\mathbf{x}_{t-1}, (1 - \alpha_t)\mathbf{I})$ ,  $t = 1, \dots, T$ , where the noise schedule  $\{\alpha_t\}_{t=1}^T$  and  $T$  is set to make  $\mathbf{x}_T$  follow approximately a standard Gaussian distribution. The reverse process can be learned to predict the noise from the corrupted data by minimizing

$$\mathcal{L}_{\text{MSE}} = \mathbb{E}_{\mathbf{x}_0, \boldsymbol{\epsilon}, t} \left[ \left\| \boldsymbol{\epsilon} - \boldsymbol{\epsilon}_\theta(\sqrt{\alpha_t}\mathbf{x}_0 + \sqrt{1 - \alpha_t}\boldsymbol{\epsilon}, t) \right\|_2^2 \right], \quad (1)$$

where the expectation is w.r.t.  $\mathbf{x}_0 \sim p(\mathbf{x})$ ,  $\boldsymbol{\epsilon} \sim \mathcal{N}(\mathbf{0}, \mathbf{I})$ , and  $t \sim \{1, \dots, T\}$ .  $\bar{\alpha}_t := \prod_{i=1}^t \alpha_i$ . Eq. 1 is equivalent to optimizing a reweighted variational bound on negative log-likelihood. Without loss of generality, in this work, we parameterize  $\boldsymbol{\epsilon}_\theta$  as the negative gradient of the energy function  $\nabla_{\mathbf{x}_t} E_\theta(\mathbf{x}_t, t)$  as in [18]. To improve the energy landscape, [5] introduced a contrastive loss

$$\mathcal{L}_{\text{Contrast}} = \mathbb{E}_{\mathbf{x}_0, \mathbf{x}_0^-, \boldsymbol{\epsilon}, t} \left[ -\log \left( \frac{e^{-E_\theta(\mathbf{x}_t, t)}}{e^{-E_\theta(\mathbf{x}_t, t)} + e^{-E_\theta(\mathbf{x}_t^-, t)}} \right) \right], \quad (2)$$

where  $\mathbf{x}_0 \sim p(\mathbf{x})$ ,  $\boldsymbol{\epsilon} \sim \mathcal{N}(\mathbf{0}, \mathbf{I})$ ,  $\mathbf{x}_t = \sqrt{\alpha_t}\mathbf{x}_0 + \sqrt{1 - \alpha_t}\boldsymbol{\epsilon}$ .  $\mathbf{x}_t^- = \sqrt{\alpha_t}\mathbf{x}_0^- + \sqrt{1 - \alpha_t}\boldsymbol{\epsilon}$ . Here  $\mathbf{x}_0^- \sim p_{\text{corrupt}}(\mathbf{x}_0^-|\mathbf{x}_0)$  are negative examples by corrupting the positive examples  $\mathbf{x}_0$ . This contrastive loss encourages the positive (ground-truth) examples to have global energy minima.

The reverse process starts with  $\mathbf{x}_T \sim \mathcal{N}(\mathbf{0}, \mathbf{I})$ , and iteratively applies the learned denoising net  $\boldsymbol{\epsilon}_\theta$ , where [19] introduces an adjustable noise scale  $\sigma_t$ :

$$\mathbf{x}_{t-1} = \frac{\sqrt{\alpha_{t-1}}\mathbf{x}_t - \sqrt{1 - \bar{\alpha}_t}\boldsymbol{\epsilon}_\theta(\mathbf{x}_t, t)}{\sqrt{\bar{\alpha}_t}} + \sqrt{1 - \bar{\alpha}_{t-1} - \sigma_t^2}\boldsymbol{\epsilon}_\theta(\mathbf{x}_t, t) + \sigma_t\boldsymbol{\epsilon}_t, \quad \boldsymbol{\epsilon}_t \sim \mathcal{N}(\mathbf{0}, \mathbf{I}). \quad (3)$$

Importantly, [19] highlights that a diffusion model trained with  $\{\alpha_t\}_{t=1}^T$  can be used to sample with  $\{\alpha_{\tau_s}\}_{s=1}^S$ , where  $\tau$  is any increasing sub-sequence of  $1, 2, \dots, T$  of length  $S$ . This variable spacing significantly accelerates sampling and will serve as an efficient approach for MCTS simulation in Section 4.3.

## 4 Method

### 4.1 Problem setup

Let  $\mathcal{D} = \{\mathcal{C}, \mathcal{X}\}$  denote a dataset for a reasoning task, where each instance consists of an input  $\mathbf{c} \in \mathbb{R}^O$  and its corresponding solution  $\mathbf{x} \in \mathbb{R}^M$ . Our goal is to model the complex reasoning problem as an optimization task to optimize an objective  $\mathcal{J}(\mathbf{c}, \mathbf{x})$  and to capitalize on the diffusion model’s ability to iteratively refine the solution  $\mathbf{x}$ .

In this work, we leverage an energy-based diffusion model to learn an energy function  $E_\theta(\mathbf{c}, \mathbf{x}_t, t)$ <sup>5</sup> to model the optimization objective  $\mathcal{J}(\mathbf{c}, \mathbf{x})$ . During inference, we apply test-time scaling by varying the number of samples and use the learned energy function as an intrinsic verifier, thereby eliminating the need for an external verifier. However, the reasoning performance gain by test-time scaling is highly dependent on both the quality of the energy landscape and the inference-time search algorithm. To address these challenges, we propose VFScale as shown in Fig. 2, with our solutions detailed in Section 4.2 and Section 4.3.

### 4.2 Training of VFScale

Although the denoising loss  $\mathcal{L}_{\text{MSE}}$  (Eq. 1) and the contrastive loss  $\mathcal{L}_{\text{Contrast}}$  (Eq. 2) are effective, we find that simply scaling up inference budget through BoN processes yields marginal gain (Sec. 5.1). Through deeper analysis, we find that the core reason is the low quality of the energy landscape, especially the lack of *performance-energy consistency*, which we address by introducing a novel Linear-Regression Negative Contrastive Learning loss and incorporating a KL regularization, which we detail as follows.

<sup>5</sup>For simplicity, we omit  $\mathbf{c}$  in subsequent notations.

**Linear-Regression Negative Contrastive Learning.** Specifically, while the contrastive loss drives positive examples to the global energy minimum, it imposes no constraints on the relative energy ordering among negative samples. For example, it is likely that a negative example  $x_t^{--}$  that is further apart from the positive example  $x_t$  has lower energy than a negative example  $x_t^-$  that is nearer. Thus, the inference process can be stuck around  $x_t^{--}$  and can hardly move out. This will result in reduced *performance-energy consistency*, where lower energy at step  $t$  does not necessarily correspond to a more accurate predicted solution  $\hat{x}_0$ , as will be shown in Sec. 5.1.

This problem can not be easily remedied by increasing inference budget through BoN during test; instead, we explore a more fundamental way to solve this problem to shape the energy landscape by regularizing the energy among negative examples during training. The approach seeks to enforce consistency between the relative energy levels of negative samples and their corresponding performance quality, comprising the following key steps:

**(1) Generate negative samples:** Specifically, from a positive example  $x_0 \sim p(x)$ , we sample two negative examples  $x_0^-$  and  $x_0^{--}$ ,<sup>6</sup> the latter has a larger L2 distance to  $x_0$ . Specifically, the distance of  $x_0$ ,  $x_0^-$  and  $x_0^{--}$  to  $x_0$  are 0,  $l_{2,0}^- = \|x_0^- - x_0\|_2$ , and  $l_{2,0}^{--} = \|x_0^{--} - x_0\|_2$ , respectively.

**(2) Obtain the energy for each sample:** Then we obtain their corresponding noisy examples at step  $t$  via  $x_t = \sqrt{\alpha_t}x_0 + \sqrt{1 - \alpha_t}\epsilon$ ,  $x_t^- = \sqrt{\alpha_t}x_0^- + \sqrt{1 - \alpha_t}\epsilon$ , and  $x_t^{--} = \sqrt{\alpha_t}x_0^{--} + \sqrt{1 - \alpha_t}\epsilon$ . Their energy are  $E_t^+ = E_\theta(x_t, t)$ ,  $E_t^- = E_\theta(x_t^-, t)$ , and  $E_t^{--} = E_\theta(x_t^{--}, t)$ , respectively.

**(3) Apply linear regression to get the slope and intercept:** To encourage a landscape where the energy difference between negative samples and the positive sample becomes smaller as they approach the positive sample, we directly constrain the relationship between the energy of different negative samples and the positive sample using linear regression. Specifically, we first apply the linear regression algorithm<sup>7</sup> to fit linear function through the three points  $\{(0, E_t^+), (l_{2,0}^-, E_t^-), (l_{2,0}^{--}, E_t^{--})\}$ , which is characterized by the slope  $k_t$  and the intercept  $b_t$ .

**(4) Calculate the LRNCL loss:** Then, we obtain the corresponding fitted points  $\{(0, \hat{E}_t^+), (l_{2,0}^-, \hat{E}_t^-), (l_{2,0}^{--}, \hat{E}_t^{--})\}$  from the linear function. We then compute the Linear-Regression Negative Contrastive Learning (LRNCL) loss as:

$$\mathcal{L}_{\text{LRNCL}} = \mathbb{E}_{x_0, x_0^-, x_0^{--}, \epsilon, t} [\max(0, \gamma - k_t) + \|E_t^+ - \hat{E}_t^+\|_2^2 + \|E_t^- - \hat{E}_t^-\|_2^2 + \|E_t^{--} - \hat{E}_t^{--}\|_2^2], \quad (4)$$

where  $\gamma$  is a hyperparameter and  $t \sim \{0, \dots, T\}$ . The first term  $\max(0, \gamma - k_t)$  encourages that any three samples  $x_t$ ,  $x_t^-$ ,  $x_t^{--}$  have a positive (and larger-than- $\gamma$ ) slope of energy vs. L2 distance. The latter three terms encourage that the energy vs. L2 distance is linear, making the energy landscape smoother.<sup>8</sup>

**KL regularization.** In addition to  $\mathcal{L}_{\text{LRNCL}}$  that improves *performance-energy consistency*, we further include KL-regularization [20] to further improve the energy landscape:

$$\mathcal{L}_{\text{KL}} = \mathbb{E}_{t, p_{\theta, t}(x)} [E_{\text{stop-grad}(\theta)}(x)] + \mathbb{E}_{t, p_{\theta, t}(x)} [\log p_{\theta, t}(x)], \quad (5)$$

where  $p_{\theta, t}(x)$  is the probability distribution of  $x_t$  at denoising step  $t$ . When optimizing w.r.t.  $\mathcal{L}_{\text{KL}}$ , it is essentially optimizing w.r.t. the sampling (denoising) process by shaping the energy landscape to make it easier to sample. The first term in  $\mathcal{L}_{\text{KL}}$  encourages the samples  $x_t$  to have low energy, and the second term is maximizing the entropy of the samples, encouraging the samples to be diverse. Both terms allow better test-time scaling. Different from [20], we have this KL regularization on each denoising step  $t$ , and we employ a more accurate estimation of the entropy [21].

Taken together, the training objective of our VFScale is:

$$\mathcal{L} = \mathcal{L}_{\text{MSE}} + \mathcal{L}_{\text{Contrast}} + \mathcal{L}_{\text{LRNCL}} + \mathcal{L}_{\text{KL}}, \quad (6)$$

where the latter two terms improve the energy landscape and boost the test-time scalability.

<sup>6</sup>Details to generate negative samples are in Appendix A.

<sup>7</sup>The details of linear regression algorithm can be found in Appendix A.

<sup>8</sup>It is also possible to use more complex shapes than linear regression to regularize the energy landscape, which we leave for future work. Here we find that simple linear regression works well.

### 4.3 Inference of VFScale

To fully harness the potential of the diffusion model with the higher-efficiency search algorithm, we propose a novel hybrid Monte Carlo Tree Search denoising (hMCTS denoising) method, which progressively applies best-of- $N$  (BoN) and Monte Carlo Tree Search (MCTS) denoising in sequence, as detailed below, throughout the denoising process. As demonstrated in Algorithm 1, we employ BoN for the diffusion process in the early diffusion stages, which introduces  $L$  initial noises to maintain a consistent number of function evaluations (NFE) per example during the diffusion process.<sup>9</sup> Subsequently, hMCTS denoising utilizes the MCTS denoising<sup>10</sup> to iteratively perform the denoising process until the termination state  $\mathbf{x}_0$  is reached. This approach enables MCTS to more accurately estimate node value when the noise is relatively small, thereby preventing the premature exclusion of potentially promising nodes. Next, we will detail the MCTS denoise process.

We treat the current diffusion state  $\mathbf{x}_t$  as the state, the noise to remove as the action, and model the denoising process of the diffusion model as a Markov Decision Process (MDP). Therefore, a *node* in MCTS represents the state  $\mathbf{x}_t$ , along with its current visit count  $N(\mathbf{x}_t)$  and state value  $Q(\mathbf{x}_t)$ . A terminal node is defined as a node whose denoising step is 0. In this context, we use  $\nabla_{\mathbf{x}_t} E_\theta(\mathbf{x}_t, t)$  and  $E_\theta(\mathbf{x}_t, t)$  of the energy-based diffusion as the policy network and value network, respectively. Each deepening of the search tree corresponds to a single denoising step. Similar to MCTS in AlphaGo [22] and AlphaZero [23], each rollout in MCTS consists of four core steps: selection, expansion, simulation, and backpropagation, as illustrated in Fig. 2 and Algorithm 1 in Appendix A:

**(1) Selection:** Based on the Upper Confidence Bound (UCB) from AlphaGo [22], starting from the current root node state  $\mathbf{x}_t$ , we select a child node based on the following adjusted UCB of MCTS-enhanced diffusion formula until a leaf node  $\{\mathbf{x}_{t'}, Q(\mathbf{x}_{t'}), N(\mathbf{x}_{t'})\}$  is reached:

$$UCB(\mathbf{x}_t, \mathbf{a}_t) = Q(\mathbf{x}_t, \mathbf{a}_t) + c \sqrt{\frac{\ln N_i}{n_i}}, \quad (7)$$

where  $Q(\mathbf{x}_t, \mathbf{a}_t)$  represent the value of children node, action  $\mathbf{a}_t$  includes predicted noise  $\epsilon_\theta$  and random Gaussian noise  $\epsilon$ ,  $n_i$  represents the number of visits to node  $i$ ,  $N_i$  represents the number of visits to the parent node of  $i$ , and  $c$  is the exploration hyperparameter.

**(2) Expansion:** Unless the state of the node reached is a terminal state  $\mathbf{x}_0$ , we expand the children of the selected node by choosing an action and creating new nodes based on the action. For the expansion step of MCTS denoising, we perform a denoising step and add different but limited Gaussian noise. This results in  $K$  distinct branches  $\{\mathbf{x}_{t'-1}^{(k)} \mid k = 0, 1, \dots, K-1\}$ , where each child node  $\mathbf{x}_{t'-1}^{(k)}$  is derived as following equation adjusted from Eq. 3 :

$$\mathbf{x}_{t'-1}^{(k)} = \sqrt{\bar{\alpha}_{t'-1}} \frac{\mathbf{x}_{t'} - \sqrt{1 - \bar{\alpha}_{t'}} \epsilon_\theta(\mathbf{x}_{t'}, t')}{\sqrt{\bar{\alpha}_{t'}}} + \sqrt{1 - \bar{\alpha}_{t'-1} - \sigma_{t'}^2} \epsilon_\theta(\mathbf{x}_{t'}, t') + \sigma_{t'} \epsilon^{(k)}, \quad (8)$$

with  $\epsilon_\theta(\mathbf{x}_{t'}, t')$  determined by  $\mathbf{x}_{t'}$  and  $t'$ , and  $\epsilon^{(k)} \sim \mathcal{N}(\mathbf{0}, \mathbf{I})$  representing random Gaussian noise.

**(3) Simulation:** We randomly select a child node and perform a random simulation of the MDP until reaching a terminal state. For the simulation of MCTS denoising, we use DDIMs [19] for fast sampling to obtain  $\hat{\mathbf{x}}_0(\mathbf{x}_{t'-1}^{(k*)})$  from the randomly chosen child node state  $\mathbf{x}_{t'-1}^{(k*)}$ , and then use  $E_\theta(\hat{\mathbf{x}}_0(\mathbf{x}_{t'-1}^{(k*)}))$  as the reward for backpropagation instead of reward from external verifier.<sup>11</sup>

**(4) Backpropagation:** Finally, we backpropagate the node values to the root node, updating the value of each node using the expected value along the path.

After  $N_r$  rollouts, we select  $\mathbf{x}_{t-1}^{(k)}$  with the largest value  $\frac{Q(\mathbf{x}_{t-1}^{(k)})}{N(\mathbf{x}_{t-1}^{(k)})}$  as the state  $\mathbf{x}_{t-1}$  for the next denoising step. The next MCTS denoising process starts from this state and proceeds until the

<sup>9</sup>In this paper, we primarily report  $K = N_r$  MCTS denoising, where ensuring  $K = N_r$ ,  $L = N_r$  guarantees that the NFE (Number of Function Evaluations) for each case of BoN, MCTS denoising, and hMCTS denoising remains the same.

<sup>10</sup>For a detailed explanation of the distinctions between hMCTS denoising, MCTS denoising, and BoN, as well as the impact of MCTS denoising start step  $t_s$ , please refer to Appendix D.

<sup>11</sup>Although our method is based on an energy-based diffusion model, the proposed hMCTS is also applicable to conventional noise-predicting diffusion models, albeit requiring an external verifier. Additional results are provided in the Appendix E.

termination state  $x_0$ . Here, the depth of the search tree is decided by three elements: the number of rollout steps  $N_r$ , the maximum number of branches  $K$  for each node, and the search policy.

To summarize, our proposed paradigm, VFScale, enhances *performance-energy consistency* and ease of sampling through LRNCL loss and KL regularization, respectively (Sec. 4.2), while fully unlocking the test-time scalability of diffusion models via hMCTS denoising (Sec. 4.3).

## 5 Experiments

In the experiments, we focus on investigating the challenges of replacing an external verifier with a learned energy function to enable test-time scaling of diffusion models via varying the number of samples. We then justify the effectiveness of our innovations in both training and inference. Specifically, we aim to address the following three key questions: (1) What factors hinder the success of test-time scaling of energy-based diffusion models? (2) Does the training of VFScale exactly improve the energy landscape to unleash the test-time scalability of diffusion models? (3) Can the inference method of VFScale achieve better test-time scaling up?

To answer these questions, we conduct extensive experiments on two challenging reasoning tasks: Maze and Sudoku. In Section 5.1, we find that the naïvely trained energy-based diffusion model [5] falls short of scaling up during test time and identify the key reason as the poor quality of the energy landscape, particularly its lack of *performance-energy consistency*. Addressing this In Section 5.2, the training methods of VFScale demonstrate a significant impact on unbinding the scalability of diffusion models. As shown in Fig. 1, with the model trained with VFScale training methods, hMCTS denoising can better release the scalability, enabling generalization to much more challenging tasks during inference (Sec. 5.3).

In Maze experiments, the datasets are generated by [24], and the diffusion model is mainly trained with Maze sizes of up to  $6 \times 6$  while tested on harder datasets with sizes significantly larger than  $6 \times 6$  (Fig. 1). For Sudoku experiments, the basic setting is adopted from [5] where the diffusion model is trained on SAT-Net dataset with 31 to 42 given entries [25] and tested on the harder RRN dataset with 17 to 34 given entries [26] with fewer given entries. All models and inference methods are evaluated with solving success rate. Here successful solving means the predicted solution exactly matches the ground-truth solution on all entries, a very stringent metric<sup>12</sup>. More experimental details can be found in Appendix B, Appendix C, and Appendix H, respectively.

All the training methods are compared with the original training pipeline in [5]. LRNCL and KL represent the loss terms  $\mathcal{L}_{\text{LRNCL}}$  and  $\mathcal{L}_{\text{KL}}$ , respectively in Eq. 6. VFScale tr. w/o LRNCL, VFScale tr. w/o KL, and VFScale tr. (ours) represent the three training methods of VFScale, the last one being the full version. **The MCTS denoising and hMCTS denoising are compared with BoN with the same computational budget.** The experiment code can be found at the repo.

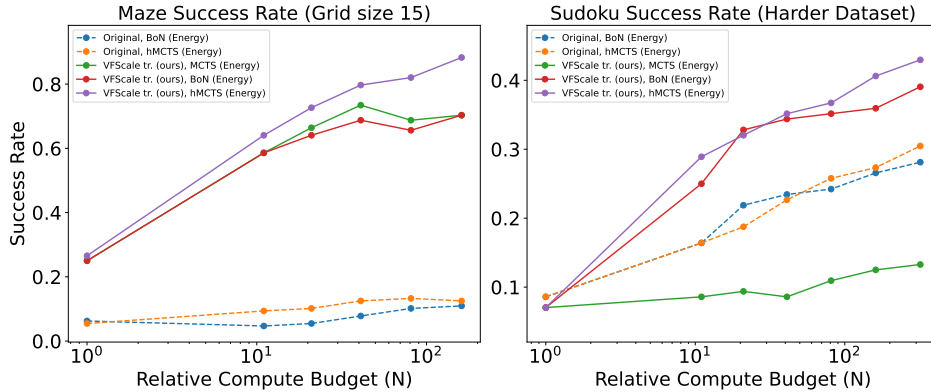


Figure 3: Scalability of different approaches on Maze and Sudoku.

<sup>12</sup>For example, a successful solving of a  $15 \times 15$  Maze needs to predict all  $31 \times 31 = 961$  entries correctly (for each grid cell, predict path/not path/wall), where the path length from start to target is on the order of  $10^2$ .

## 5.1 Test-Time Scaling bottleneck of energy-based diffusion models

**Test-time scaling up the diffusion model to solve harder reasoning problems is challenging.** When tested on more challenging tasks, diffusion models trained with the original method fail to achieve substantial gains, even under larger inference budgets. Specifically, as shown in Table 1, models trained on simpler tasks with original training methods exhibit significantly poorer performance on more complex tasks. Success rate plunges from 100% on Maze size  $6 \times 6$  to 6% on  $15 \times 15$ , and from 32% on Sudoku with 33 given entries to below 5% at 25 and 0% at 21 givens. Building upon this, we conduct best-of- $N$  to examine whether test-time scaling can enhance the performance of the originally trained model. Table 3’s “Original, BoN” row reveals that enlarging the inference budget  $N$  offers marginal gains—Maze success climbs by at most 5%, while Sudoku remains below 30% even at  $N = 320$ . These indicate that naïve test-time scaling of diffusion models fails to deliver meaningful improvements. Next, we analyze the underlying causes from the perspectives of training and inference, respectively.

Table 1: Success rate across different grid sizes of Maze and various number of given entries for naïve inference ( $N = 1$ ) for comparison of the generalization ability of models obtained by different training methods. Let  $M$  denote the grid size of Maze and  $D$  denote the number of given digits in Sudoku. Original denotes the original training method in [5]. VFScale tr. (ours) denotes the training method of VFScale, and all subsequent descriptions will follow this definition. Bold font denotes the best model, and an underline denotes the second-best model. The same markings are used in the tables below.

Methods	Maze success rate					Sudoku success rate				
	$M = 6$	$M = 8$	$M = 10$	$M = 12$	$M = 15$	$D = 33$	$D = 29$	$D = 25$	$D = 21$	$D = 17$
Original	1.0000	0.9062	0.5781	0.3750	0.0625	0.3203	0.1094	0.0234	0.0000	0.0000
VFScale tr. w/o LRNCL	1.0000	<u>0.9922</u>	<u>0.7734</u>	<b>0.5625</b>	0.2500	<b>0.4219</b>	<u>0.1719</u>	<b>0.0469</b>	<b>0.0078</b>	0.0000
VFScale tr. w/o KL	1.0000	0.9844	0.6953	0.4375	<b>0.2812</b>	<b>0.4219</b>	<b>0.2578</b>	<u>0.0391</u>	<b>0.0078</b>	0.0000
VFScale tr. (ours)	1.0000	<b>1.0000</b>	<b>0.7750</b>	<u>0.5391</u>	<b>0.2812</b>	0.1953	0.1016	0.0078	0.0000	0.0000

Table 2: Success rate of BoN for different training methods on Maze with grid size **15** and Sudoku harder dataset guided with ground truth. Here,  $L = N$ .

Methods	Maze success rate						Sudoku success rate						
	$N=1$	$N=11$	$N=21$	$N=41$	$N=81$	$N=161$	$N=1$	$N=11$	$N=21$	$N=41$	$N=81$	$N=161$	$N=321$
Original, BoN (Energy)	0.0625	0.0469	0.0547	0.0781	0.1016	0.1094	0.0859	0.1641	0.2188	0.2344	0.2422	0.2656	0.2812
Original, BoN (Ground Truth)	0.0625	0.1250	0.1094	0.1328	0.1719	0.1719	0.0859	0.1641	0.2188	0.2344	0.2422	0.2656	0.2969
VFScale tr. w/o LRNCL, BoN (Ground Truth)	<b>0.2500</b>	<b>0.5078</b>	<b>0.5938</b>	<b>0.6562</b>	<b>0.7109</b>	<b>0.7422</b>	<b>0.1094</b>	<b>0.2578</b>	<b>0.2969</b>	<b>0.3438</b>	<b>0.3750</b>	<b>0.3828</b>	<b>0.4219</b>

**First, there is still considerable room for improvement on the training side to fully unlock the test-time scalability of diffusion models.** As shown in Table 2, even when ground truth is used to guide test-time scaling, the success rate on the Maze task increases by only 7% over the energy-guided scaling method at an inference budget of  $N = 161$ , remaining below 20%. On the Sudoku task, raising  $N$  to 321 yields under a 2% improvement compared with energy-guided scaling, still below 30%. These findings indicate that employing the learned energy function as the verifier can lead to misestimation; the *performance–energy consistency* must be further improved. Moreover, Table 4 reports that the originally trained model achieves only about 70% *performance–energy consistency* in quantitative evaluation, underscoring a significant mismatch between the energy-based verifier and actual performance. In short, these results highlight the urgent need to refine training methods to improve the quality of energy landscape.

**Second, substantial advancements in test-time scaling methodologies are still required to fully harness the inherent scalability of diffusion models.** As shown in Table 2’s first and second rows, regardless of whether ground truth is as a verifier, the performance of BoN quickly plateaus. On the Maze task, increasing the inference budget  $N$  from 1 to 161 raises the success rate from 6% to 17%—a gain of only 10%—and the rate of improvement slows markedly; a similar trend is observed on Sudoku, where success rate growth decelerates significantly and the maximum success rate remains below 30%. These findings suggest that there remains substantial room to enhance the efficiency of test-time scaling methods.

## 5.2 The effect of VFScale training methods

In this subsection, we evaluate the effectiveness of the LRNCL and KL losses in VFScale compared with the baseline model trained without these losses. **First**, as shown in Table 3’s “ $N=1$ ” columns,



Table 3: Success rate on Maze with grid size **15** and Sudoku harder dataset for comparison of the model’s ability to scale up under BoN with different training methods. Here,  $L = N$ .

Methods	Maze success rate						Sudoku success rate						
	$N=1$	$N=11$	$N=21$	$N=41$	$N=81$	$N=161$	$N=1$	$N=11$	$N=21$	$N=41$	$N=81$	$N=161$	$N=321$
Original, BoN	0.0625	0.0469	0.0547	0.0781	0.1016	0.1094	0.0859	0.1641	0.2188	0.2344	0.2422	0.2656	0.2812
VFScale tr. w/o LRNCL, BoN	0.2500	0.4297	0.5000	0.5391	0.6016	0.6094	0.1172	<b>0.2656</b>	0.3125	<b>0.3438</b>	<b>0.3750</b>	<b>0.3906</b>	<b>0.4141</b>
VFScale tr. w/o KL, BoN	<b>0.2812</b>	0.4688	0.4922	0.5547	0.5859	0.6250	<b>0.1562</b>	0.2422	0.2578	0.2656	0.2656	0.2891	0.3047
VFScale tr. (ours), BoN	0.2656	<b>0.5859</b>	<b>0.6406</b>	<b>0.6875</b>	<b>0.6562</b>	<b>0.7031</b>	0.0703	0.2500	<b>0.3281</b>	<b>0.3438</b>	0.3516	0.3594	0.3906

Table 4: *Performance-energy consistency* of BoN on Maze with grid size 15 to test the effect of LRNCL loss. Here,  $L = N$ . Details of consistency calculation can be found in Appendix A.

Methods	Performance-energy consistency				
	$N=11$	$N=21$	$N=41$	$N=81$	$N=161$
Original, BoN	0.7317	0.7333	0.7313	0.7283	0.7300
VFScale tr. w/o KL, BoN	<b>0.8370</b>	<b>0.8445</b>	<b>0.8476</b>	<b>0.8375</b>	<b>0.8371</b>

even without test-time scaling, integrating either the LRNCL loss or the KL loss produces significant improvements: on the Maze task, the success rate rises from 6% to 28%, and on Sudoku it likewise increases from 9% to 16%. **Second**, Table 4 also shows that adding the LRNCL loss alone produces a steady improvement in *performance-energy consistency* of over 10%. **Finally**, when we apply BoN for test-time scaling of the diffusion model, Table 3 demonstrates that using only the LRNCL loss, only the KL loss, or both, boosts the Maze success rate by more than 60% and the Sudoku success rate by over 10%. Meanwhile, as illustrated in the Fig. 4, after incorporating the LRNCL loss and the KL loss, the solutions produced by the model at different denoising steps are all noticeably closer to the ground truth solutions. Together, these findings provide strong evidence that the LRNCL and KL losses significantly enhance the test-time scalability of diffusion models.

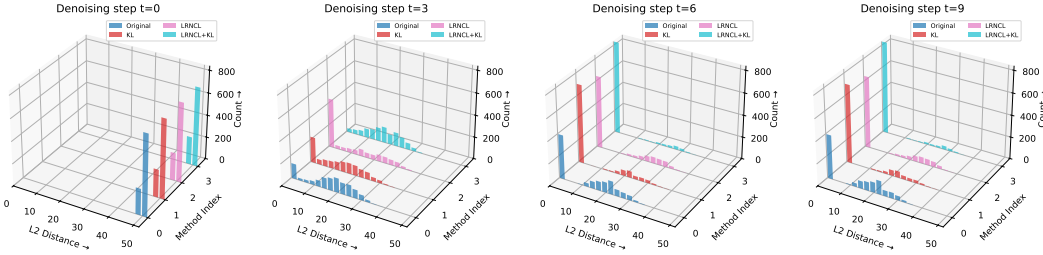


Figure 4: Comparison of the L2 distances between the solutions obtained by different training methods and the ground truth at various denoising steps.

### 5.3 Test-time Scalability of VFScale

Table 5: Success rate of different approaches on Maze with grid size **15** and Sudoku harder dataset. Here,  $N_r = N$ ,  $K = N$ ,  $L = N$ .

Methods	Maze success rate						Sudoku success rate						
	$N=1$	$N=11$	$N=21$	$N=41$	$N=81$	$N=161$	$N=1$	$N=11$	$N=21$	$N=41$	$N=81$	$N=161$	$N=321$
Original, BoN	0.0625	0.0469	0.0547	0.0781	0.1016	0.1094	<b>0.0859</b>	0.1641	0.2188	0.2344	0.2422	0.2656	0.2812
Original, hMCTS denoising (ours)	0.0625	0.0938	0.1016	0.1250	0.1328	0.1250	<b>0.0859</b>	0.1641	0.1875	0.2266	0.2578	0.2734	0.3047
VFScale tr. (ours), MCTS denoising (ours)	0.2656	0.5859	0.6641	0.7344	0.6875	0.7031	0.0703	0.0859	0.0938	0.0859	0.1094	0.1250	0.1328
VFScale tr. (ours), BoN	0.2656	0.5859	0.6406	0.6875	0.6562	0.7031	0.0703	0.2500	<b>0.3281</b>	<b>0.3438</b>	0.3516	0.3594	0.3906
VFScale tr. (ours), hMCTS denoising (ours)	<b>0.2656</b>	<b>0.6406</b>	<b>0.7266</b>	<b>0.7969</b>	<b>0.8203</b>	<b>0.8828</b>	0.0703	<b>0.2891</b>	0.3203	0.3516	<b>0.3672</b>	<b>0.4062</b>	<b>0.4297</b>

Using the diffusion model trained with VFScale training methods, we evaluate various inference approaches to validate the efficacy of our inference methods described in Section 4.3. As shown in Table 5, in the Maze experiment, the MCTS denoising method slightly outperforms BoN, while our hMCTS denoising yields a significantly higher success rate, with a maximum improvement of approximately 18% than BoN. Moreover, as the budget  $N$  increases, the performance gap between hMCTS denoising and BoN widens. In the Sudoku experiment, hMCTS denoising also consistently outperforms BoN, with a maximum improvement of 5%. As illustrated in the *scaling curve* in Fig. 3,

hMCTS denoising with the model trained with additional LRNCL loss and KL loss shows a marked improvement compared to both other inference methods. At the same time, the rate of improvement for other inference methods clearly slows down compared to hMCTS denoising. These results provide strong evidence that our inference method can effectively scale up during test time, offering a clear advantage over BoN.

## 6 Conclusion

In this work, we have introduced the Verifier-free Test-time Scalable Diffusion Model (VFScale), a novel framework to achieve scalable intrinsic reasoning to tackle more complex reasoning tasks than in training. VFScale explores applying the varying number-of-sample scaling method with learned energy as a verifier. Concretely, faced with a low-quality energy landscape and lack of efficient search algorithms, VFScale is composed of two innovations on training and inference to address these challenges. On the training side, VFScale introduces two auxiliary training losses,  $\mathcal{L}_{\text{LRNCL}}$  and  $\mathcal{L}_{\text{KL}}$ , to improve the energy landscape. This, in turn, ensures that using the learned energy function as a verifier is effective for test-time scaling. On the inference side, VFScale integrates hybrid Monte Carlo Tree Search (hMCTS) denoising to better leverage the model’s test-time scalability. We have conducted extensive experiments on Maze and Sudoku to validate the efficacy of VFScale and believe that VFScale offers a robust solution for test-time scaling, unlocking the notable potential of diffusion models for complex reasoning. Limitations and future directions are discussed in Appendix G.

## References

- [1] Daniel Kahneman. *Thinking, fast and slow*. macmillan, 2011.
- [2] Hunter Lightman, Vineet Kosaraju, Yuri Burda, Harrison Edwards, Bowen Baker, Teddy Lee, Jan Leike, John Schulman, Ilya Sutskever, and Karl Cobbe. Let’s verify step by step. In *The Twelfth International Conference on Learning Representations*, 2023.
- [3] DeepSeek-AI, Daya Guo, Dejian Yang, Haowei Zhang, Junxiao Song, Ruoyu Zhang, Runxin Xu, Qihao Zhu, Shirong Ma, Peiyi Wang, Xiao Bi, Xiaokang Zhang, Xingkai Yu, Yu Wu, Z. F. Wu, Zhibin Gou, Zhihong Shao, Zhuoshu Li, Ziyi Gao, Aixin Liu, Bing Xue, Bingxuan Wang, Bochao Wu, Bei Feng, Chengda Lu, Chenggang Zhao, Chengqi Deng, Chenyu Zhang, Chong Ruan, Damai Dai, Deli Chen, Dongjie Ji, Erhang Li, Fangyun Lin, Fucong Dai, Fuli Luo, Guangbo Hao, Guanting Chen, Guowei Li, H. Zhang, Han Bao, Hanwei Xu, Haocheng Wang, Honghui Ding, Huajian Xin, Huazuo Gao, Hui Qu, Hui Li, Jianzhong Guo, Jiashi Li, Jiawei Wang, Jingchang Chen, Jingyang Yuan, Junjie Qiu, Junlong Li, J. L. Cai, Jiaqi Ni, Jian Liang, Jin Chen, Kai Dong, Kai Hu, Kaige Gao, Kang Guan, Kexin Huang, Kuai Yu, Lean Wang, Lecong Zhang, Liang Zhao, Litong Wang, Liyue Zhang, Lei Xu, Leyi Xia, Mingchuan Zhang, Minghua Zhang, Minghui Tang, Meng Li, Miaojuan Wang, Mingming Li, Ning Tian, Panpan Huang, Peng Zhang, Qiancheng Wang, Qinyu Chen, Qiushi Du, Ruiqi Ge, Ruisong Zhang, Ruizhe Pan, Runji Wang, R. J. Chen, R. L. Jin, Ruyi Chen, Shanghao Lu, Shangyan Zhou, Shanhuang Chen, Shengfeng Ye, Shiyu Wang, Shuiping Yu, Shunfeng Zhou, Shuting Pan, S. S. Li, Shuang Zhou, Shaoqing Wu, Shengfeng Ye, Tao Yun, Tian Pei, Tianyu Sun, T. Wang, Wangding Zeng, Wanbiao Zhao, Wen Liu, Wenfeng Liang, Wenjun Gao, Wenqin Yu, Wentao Zhang, W. L. Xiao, Wei An, Xiaodong Liu, Xiaohan Wang, Xiaokang Chen, Xiaotao Nie, Xin Cheng, Xin Liu, Xin Xie, Xingchao Liu, Xinyu Yang, Xinyuan Li, Xuecheng Su, Xuheng Lin, X. Q. Li, Xiangyue Jin, Xiaojin Shen, Xiaosha Chen, Xiaowen Sun, Xiaoxiang Wang, Xinnan Song, Xinyi Zhou, Xianzu Wang, Xinxia Shan, Y. K. Li, Y. Q. Wang, Y. X. Wei, Yang Zhang, Yanhong Xu, Yao Li, Yao Zhao, Yaofeng Sun, Yaohui Wang, Yi Yu, Yichao Zhang, Yifan Shi, Yiliang Xiong, Ying He, Yishi Piao, Yisong Wang, Yixuan Tan, Yiyang Ma, Yiyuan Liu, Yongqiang Guo, Yuan Ou, Yudian Wang, Yue Gong, Yuheng Zou, Yujia He, Yunfan Xiong, Yuxiang Luo, Yuxiang You, Yuxuan Liu, Yuyang Zhou, Y. X. Zhu, Yanhong Xu, Yanping Huang, Yaohui Li, Yi Zheng, Yuchen Zhu, Yunxian Ma, Ying Tang, Yukun Zha, Yuting Yan, Z. Z. Ren, Zehui Ren, Zhangli Sha, Zhe Fu, Zhean Xu, Zhenda Xie, Zhengyan Zhang, Zhewen Hao, Zhicheng Ma, Zhigang Yan, Zhiyu Wu, Zihui Gu, Zijia Zhu, Zijun Liu, Zilin Li, Ziwei Xie, Ziyang Song, Zizheng Pan, Zhen Huang, Zhipeng Xu, Zhongyu Zhang, and Zhen Zhang. Deepseek-r1: Incentivizing reasoning capability in llms via reinforcement learning, 2025.

- [4] Yilun Du, Shuang Li, Joshua Tenenbaum, and Igor Mordatch. Learning iterative reasoning through energy minimization. In *International Conference on Machine Learning*, pages 5570–5582. PMLR, 2022.
- [5] Yilun Du, Jiayuan Mao, and Joshua B Tenenbaum. Learning iterative reasoning through energy diffusion. *arXiv preprint arXiv:2406.11179*, 2024.
- [6] Nanye Ma, Shangyuan Tong, Haolin Jia, Hexiang Hu, Yu-Chuan Su, Mingda Zhang, Xuan Yang, Yandong Li, Tommi Jaakkola, Xuhui Jia, and Saining Xie. Inference-time scaling for diffusion models beyond scaling denoising steps, 2025.
- [7] Long Ouyang, Jeffrey Wu, Xu Jiang, Diogo Almeida, Carroll Wainwright, Pamela Mishkin, Chong Zhang, Sandhini Agarwal, Katarina Slama, Alex Ray, et al. Training language models to follow instructions with human feedback. *Advances in neural information processing systems*, 35:27730–27744, 2022.
- [8] Harrison Lee, Samrat Phatale, Hassan Mansoor, Thomas Mesnard, Johan Ferret, Kellie Ren Lu, Colton Bishop, Ethan Hall, Victor Carbune, Abhinav Rastogi, et al. Rlaif vs. rlhf: Scaling reinforcement learning from human feedback with ai feedback. In *International Conference on Machine Learning*, pages 26874–26901. PMLR, 2024.
- [9] Tania Lombrozo. Learning by thinking in natural and artificial minds. *Trends in Cognitive Sciences*, 2024.
- [10] Michelene TH Chi, Nicholas De Leeuw, Mei-Hung Chiu, and Christian LaVancher. Eliciting self-explanations improves understanding. *Cognitive science*, 18(3):439–477, 1994.
- [11] Jie Huang, Xinyun Chen, Swaroop Mishra, Huaixiu Steven Zheng, Adams Wei Yu, Xinying Song, and Denny Zhou. Large language models cannot self-correct reasoning yet. In *The Twelfth International Conference on Learning Representations*.
- [12] Yang Song, Jascha Sohl-Dickstein, Diederik P Kingma, Abhishek Kumar, Stefano Ermon, and Ben Poole. Score-based generative modeling through stochastic differential equations. *arXiv preprint arXiv:2011.13456*, 2020.
- [13] Amrith Setlur, Nived Rajaraman, Sergey Levine, and Aviral Kumar. Scaling test-time compute without verification or rl is suboptimal, 2025.
- [14] Charlie Snell, Jaehoon Lee, Kelvin Xu, and Aviral Kumar. Scaling llm test-time compute optimally can be more effective than scaling model parameters, 2024.
- [15] Jonathan Ho, Ajay Jain, and Pieter Abbeel. Denoising diffusion probabilistic models. *Advances in neural information processing systems*, 33:6840–6851, 2020.
- [16] Tero Karras, Miika Aittala, Timo Aila, and Samuli Laine. Elucidating the design space of diffusion-based generative models. *Advances in neural information processing systems*, 35:26565–26577, 2022.
- [17] Jaesik Yoon, Hyeonseo Cho, Doojin Baek, Yoshua Bengio, and Sungjin Ahn. Monte carlo tree diffusion for system 2 planning, 2025.
- [18] Yilun Du, Conor Durkan, Robin Strudel, Joshua B Tenenbaum, Sander Dieleman, Rob Fergus, Jascha Sohl-Dickstein, Arnaud Doucet, and Will Sussman Grathwohl. Reduce, reuse, recycle: Compositional generation with energy-based diffusion models and mcmc. In *International conference on machine learning*, pages 8489–8510. PMLR, 2023.
- [19] Jiaming Song, Chenlin Meng, and Stefano Ermon. Denoising diffusion implicit models. In *International Conference on Learning Representations*.
- [20] Yilun Du, Shuang Li, Joshua Tenenbaum, and Igor Mordatch. Improved contrastive divergence training of energy-based models. In *International Conference on Machine Learning*, pages 2837–2848. PMLR, 2021.
- [21] Damiano Lombardi and Sanjay Pant. Nonparametric k-nearest-neighbor entropy estimator. *Physical Review E*, 93(1):013310, 2016.

- [22] David Silver, Aja Huang, Chris J Maddison, Arthur Guez, Laurent Sifre, George Van Den Driessche, Julian Schrittwieser, Ioannis Antonoglou, Veda Panneershelvam, Marc Lanctot, et al. Mastering the game of go with deep neural networks and tree search. *nature*, 529(7587):484–489, 2016.
- [23] David Silver, Julian Schrittwieser, Karen Simonyan, Ioannis Antonoglou, Aja Huang, Arthur Guez, Thomas Hubert, Lucas Baker, Matthew Lai, Adrian Bolton, et al. Mastering the game of go without human knowledge. *nature*, 550(7676):354–359, 2017.
- [24] Michael Igorevich Ivanitskiy, Rusheb Shah, Alex F Spies, Tilman Räuher, Dan Valentine, Can Rager, Lucia Quirke, Chris Mathwin, Guillaume Corlouer, Cecilia Diniz Behn, et al. A configurable library for generating and manipulating maze datasets. *arXiv preprint arXiv:2309.10498*, 2023.
- [25] Po-Wei Wang, Priya Donti, Bryan Wilder, and Zico Kolter. Satnet: Bridging deep learning and logical reasoning using a differentiable satisfiability solver. In *International Conference on Machine Learning*, pages 6545–6554. PMLR, 2019.
- [26] Rasmus Palm, Ulrich Paquet, and Ole Winther. Recurrent relational networks. *Advances in neural information processing systems*, 31, 2018.
- [27] David Lane, David Scott, Mikki Hebl, Rudy Guerra, Dan Osherson, and Heidi Zimmer. *Introduction to statistics*. Citeseer, 2003.
- [28] Yangzhen Wu, Zhiqing Sun, Shanda Li, Sean Welleck, and Yiming Yang. Inference scaling laws: An empirical analysis of compute-optimal inference for problem-solving with language models. *arXiv preprint arXiv:2408.00724*, 2024.

## A Related algorithms and metric caculation

### A.1 Performance-energy Consistency

From a high-level perspective, higher performance–energy consistency indicates that the learned energy function serves as a more accurate intrinsic verifier; conversely, lower consistency denotes less precise verification. In this paper, performance-energy consistency refers to the consistency between the results evaluated using an energy model and those evaluated using real-world metrics for the same sample. Specifically, the consistency requires that good samples are assigned low energy, while poor samples are assigned high energy. Performance-energy consistency measures the proportion of element pairs that maintain the same relative order in both permutations  $X$  and  $Y$ , where  $X$  and  $Y$  represent the index arrays obtained by sorting the original energy values  $\mathbf{E} = (E_1, E_2, \dots, E_N)$  and performance metric values  $\mathbf{P} = (P_1, P_2, \dots, P_N)$ , respectively, in ascending order. In this paper, the energy values are calculated by energy model  $E_\theta(x_0)$  for samples  $x_0$ . The performance metric values are calculated as the L2 distance between the generated samples  $x_0$  and the ground truth under the given condition.

Let  $X = (X_1, X_2, \dots, X_N)$  and  $Y = (Y_1, Y_2, \dots, Y_N)$  be the index arrays obtained by sorting the original energy values  $\mathbf{E} = (E_1, E_2, \dots, E_N)$  and performance metric values  $\mathbf{P} = (P_1, P_2, \dots, P_N)$ , respectively, in ascending order. Specifically,  $X_i$  is the rank of the  $i$ -th sample in the sorted energy values  $\mathbf{E}$ , and  $Y_i$  is the rank of the  $i$ -th sample in the sorted performance metric values  $\mathbf{P}$ .

**Consistency Definition:** The **consistency** is defined as the proportion of consistent pairs  $(i, j)$  where  $i < j$  and the relative order of  $i$  and  $j$  in  $X$  is the same as in  $Y$ . Specifically:

$$\text{Consistency} = \frac{1}{\binom{N}{2}} \sum_{i=1}^{N-1} \sum_{j=i+1}^N \mathbb{I}((X_i < X_j \wedge Y_i < Y_j) \vee (X_i > X_j \wedge Y_i > Y_j)),$$

where:

- $\binom{N}{2} = \frac{N(N-1)}{2}$  is the total number of pairs  $(i, j)$  with  $i < j$ ,
- $\mathbb{I}[\cdot]$  is the indicator function, which evaluates to 1 if the condition inside the brackets holds (i.e., the relative order is consistent), and 0 otherwise.

### A.2 Negative Sample Generation

Negative samples are generated by introducing noise into the positive sample  $x_0$ . In the Maze and Sudoku experiments, permutation noise is applied to the channel dimension to induce significant changes in the solution. Other noise types can be used, as this remains a hyperparameter choice. Specifically, we first randomly sample two scalars  $p_1$  and  $p_2$  from a uniform distribution in the interval  $[0, 1]$ , i.e.,  $p_1, p_2 \sim \text{Uniform}(0, 1)$  ( $p_1 < p_2$ ). Then, for each channel position of the positive sample  $x_0$ , we swap the channel positions with probabilities  $p_1$  and  $p_2$ , resulting in  $x_0^-$  and  $x_0^{--}$ , such that the L2 distance between  $x_0^-$  and  $x_0$  is smaller than the L2 distance between  $x_0^{--}$  and  $x_0$ . For other noise types, such as Gaussian noise, we normalize the L2 norm of the noise and apply noise at different scales to ensure that the L2 distance from  $x_0^-$  to  $x_0$  is smaller than the L2 distance from  $x_0^{--}$  to  $x_0$ .

### A.3 Linear-regression algorithm

Given three points  $(x_1, y_1)$ ,  $(x_2, y_2)$ , and  $(x_3, y_3)$ , we wish to fit a line of the form [27]:

$$y = kx + b$$

The mean of the  $x$ -coordinates and the mean of the  $y$ -coordinates are:

$$\bar{x} = \frac{1}{3}(x_1 + x_2 + x_3), \quad \bar{y} = \frac{1}{3}(y_1 + y_2 + y_3)$$

The slope  $k$  of the best-fit line is given by the formula:

$$k = \frac{\sum_{i=1}^3 (x_i - \bar{x})(y_i - \bar{y})}{\sum_{i=1}^3 (x_i - \bar{x})^2}$$

---

**Algorithm 1** hMCTS denoising of VFScale

---

```
1: Input: EBM  $E_\theta(\cdot)$ , Diffusion Steps  $T$ , MCTS denoising start step  $t_s$ , Number of
   initial noise for Best-of-N  $L$ , Maximum MCTS branch count  $K$ , Maximum MCTS
   rollout step  $N_r$ , A set of initial diffusion state  $\{\mathbf{x}_T^{(k)} \mid k = 1, \dots, L\}$  sampled from
   Gaussian noise.
2: // BoN for  $T \rightarrow t_s$ 
3: for  $t = T$  to  $t_s$  do
4:   Use Eq. 3 to get  $\mathbf{x}_{t-1}^{(k)}$  for  $k = 1, \dots, L$ 
5: end for
    $\mathbf{x}_{t_s} \leftarrow \arg \min_{\mathbf{x}_{t_s}^{(k)}} E_\theta(\mathbf{x}_{t_s}^{(k)})$ 
6: // MCTS denoising for  $t_s \rightarrow 1$ 
7: for  $t = t_s$  to 1 do
8:   // Do MCTS Rollouts:
9:   for  $i = 1$  to  $N_r$  do
10:    Selection: Use UCB from Eq. 7 to select the child node until a leaf node or a
       terminal node  $\{\mathbf{x}_{t'}, Q(\mathbf{x}_{t'}), N(\mathbf{x}_{t'})\}$  is reached and form a path using the nodes
       accessed during the selection;
11:    Expansion: Use Eq. 8 to generate child node state  $\mathbf{x}_{t'-1}^{(k)}$  for  $\mathbf{x}_{t'}$  and initialize
        $Q(\mathbf{x}_{t'-1}^{(k)}) = 0, N(\mathbf{x}_{t'-1}^{(k)}) = 0$  for  $k = 0, \dots, K - 1$ ;
12:    Simulation: Randomly choose  $k^* \sim \{0, \dots, K - 1\}$  and do DDIM simulation
       from  $\mathbf{x}_{t'-1}^{(k^*)}$  to get  $\hat{\mathbf{x}}_0(\mathbf{x}_{t'-1}^{(k^*)})$ ;
13:    Backpropagation: Update the value and visit count of each node  $\mathbf{x}_{t_p}$  in the path
       using  $Q(\mathbf{x}_{t_p}) \leftarrow Q(\mathbf{x}_{t_p}) - E_\theta(\hat{\mathbf{x}}_0(\mathbf{x}_{t'-1}^{(k^*)}))$ ;
14:     $N(\mathbf{x}_{t_p}) \leftarrow N(\mathbf{x}_{t_p}) + 1$ ;
15:   end for
16:    $\mathbf{x}_{t-1} \leftarrow \arg \max_{\mathbf{x}_{t-1}^{(k)}} \frac{Q(\mathbf{x}_{t-1}^{(k)})}{N(\mathbf{x}_{t-1}^{(k)})}$ 
17: end for
18: return  $\mathbf{x}_0$ 
```

---

This formula represents the least-squares solution for the slope. Once the slope  $k$  is determined, the intercept  $b$  can be calculated as:

$$b = \bar{y} - k\bar{x}$$

The equation of the best-fit line is:

$$\hat{y} = kx + b$$

#### A.4 Inference algorithm

Detailed algorithm of hMCTS of VFScale inference method is in Algorithm 1.

## B Details of experiments

### B.1 Core Metric Definition

For Maze, successful solving means finding a continuous path from starting location to target location without any breaking or overlapping with the wall; for Sudoku, successful solving means filling all the missing numbers that *exactly* match the ground-truth, both of which are very stringent metrics.

### B.2 Details of Sudoku experiments

For Sudoku experiment, the dataset, model architecture, and training configurations are adopted from [5]. We mainly use solving success rate to evaluate different models. Model backbone and training configurations can be found in Fig. 5 and Table 6, respectively. All the exploration hyperparameters  $c$  are set as 100 for Sudoku task.

3x3 Conv2D, 384
Resblock 384
Resblock 384
Resblock 384
Resblock 384
Resblock 384
Resblock 384
3x3 Conv2D, 9

Figure 5: The model architecture for VFScale on Sudoku task. The energy value is computed using the L2 norm of the final predicted output similar to [18], while the output is directly used as noise prediction for the diffusion baseline.

Table 6: **Details of training for Sudoku task.**

Training configurations	
Number of training steps	100000
Training batch size	64
Learning rate	0.0001
Diffusion steps	10
Inner loop optimization steps	20
Denoising loss type	MSE
Optimizer	Adam

### B.3 Details of Maze experiments

The details of maze experiments and model backbone are provided in Table 7 and Fig. 6, respectively. The key metric, the maze-solving success rate is defined as the proportion of model-generated paths that have no breakpoints, do not overlap with walls, and begin and end at the start and target points, respectively. Maze datasets are generated by [24], and detailed hyperparameter configurations are in Table 7. All the exploration hyperparameters  $c$  are set as 100 for Maze task.

3x3 Conv2D, 384
Resblock 384
Resblock 384
Resblock 384
Resblock 384
Resblock 384
Resblock 384
3x3 Conv2D, 9

Figure 6: The model architecture for VFScale on Maze task. The energy value is computed using the L2 norm of the final predicted output similar to [18], while the output is directly used as noise prediction for the diffusion baseline.

### B.4 Compute Resources

For training efficiency, we report the training time of our models along with the machine information (1 GPU with 80 GB of VRAM, CPU: 16). On the Maze (100,000 steps) environment, naive training took 2 hours, while incorporating LRNCL increased the training time to 4 hours. Adding KL

Table 7: **Details of Maze dataset, training.**

Dataset:	
Size of training dataset with grid size 4	10219
Size of training dataset with grid size 5	9394
Size of training dataset with grid size 6	10295
Minimum length of solution path	5
Algorithm to generate the maze	DFS
Size of test dataset with grid size 6	837
Size of test dataset with grid size 8	888
Size of test dataset with grid size 10	948
Size of test dataset with grid size 12	960
Size of test dataset with grid size 15	975
Size of test dataset with grid size 20	978
Size of test dataset with grid size 30	994
Training configurations	
Number of training steps	200000
Training batch size	64
Learning rate	0.0001
Diffusion steps	10
Inner loop optimization steps	20
Denoising loss type	MSE + MAE
Optimizer	Adam

regularization resulted in a 3-hour training time, and combining LRNCL and KL required 6 hours. For the Sudoku (200,000 steps) environment, naive training took 4 hours. Training with +LRNCL took 5 hours, +KL took 6 hours, and +LRNCL+KL required 7 hours.

## C Performance sensitivity to hyperparameters

In this subsection, we analyze the impact of several hyperparameters on the experimental results. As shown in Table 9, the influence of different noise scales on the performance of various methods is presented. The hMCTS denoising and BoN require a relatively larger noise scale to better expand the search space and improve final performance, while the diffusion model with naive inference performs best with a smaller noise scale. As demonstrated in Table 8 and Fig. 7, the effect of varying inner-loop optimization steps on the results is also analyzed. It can be observed that performance improves gradually with an increasing number of steps, and after 5 steps, the performance stabilizes and the improvement slows down. Therefore, we chose 5 inner-loop optimization steps for the Maze experiments in this paper.

Table 8: Success rate across the different number of inner-loop optimization step on Maze with grid size **15**.

Methods	Number of optimization step									
	1	2	3	4	5	6	7	8	9	10
VFScale tr. (ours), Naive inference	0.0000	0.1562	0.2109	0.2734	0.2812	0.2734	0.2812	0.2969	0.2969	0.2969

Table 9: Success rate across different noise scales on Maze with grid size **15**.

Methods	Noise scale									
	0.1	0.2	0.3	0.4	0.5	0.6	0.7	0.8	0.9	1.0
VFScale tr. (ours), hMCTS denoising (energy)	0.3828	0.4375	0.5312	0.6094	0.6562	0.6953	0.7031	0.7344	0.7734	0.7969
VFScale tr. (ours), naive inference	0.3125	0.2656	0.2578	0.2344	0.2422	0.2656	0.2578	0.2422	0.2500	0.2500
VFScale tr. (ours), BoN(energy)	0.3906	0.4453	0.5312	0.5703	0.5938	0.6328	0.6641	0.6719	0.6797	0.6562



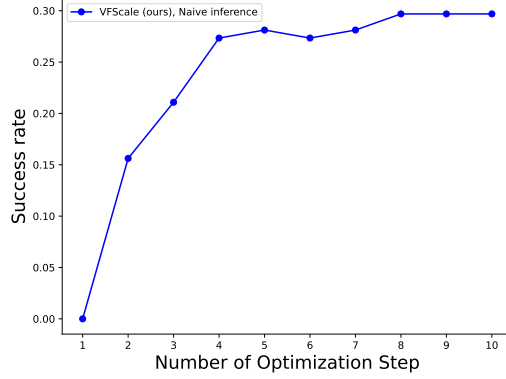


Figure 7: Visualization of success rate across different number of inner-loop optimization steps on Maze with grid size  $15 \times 15$ .

## D Additional results

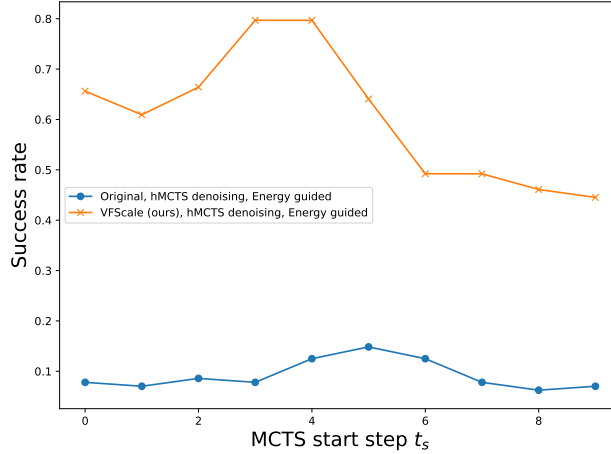


Figure 8: Visualization of Success rate across different MCTS start step  $t_s$ .

The parameter  $t_s$  controls the proportion of the total inference budget allocated to MCTS denoising. When  $t_s = 9$ , it means only MCTS denoising is used, while  $t_s = 0$  means only BoN is employed. For  $0 < t_s < 9$ , hMCTS denoising is applied. As shown in Table 10 and Fig. 8, there is a noticeable peak in model performance as  $t_s$  varies.

Table 10: Success rate of hMCTS denoising on Maze with grid size **15** across different MCTS start steps.

Methods	0	1	2	3	4	5	6	7	8	9
Original, hMCTS denoising (energy)	0.0781	0.0703	0.0859	0.0781	0.1250	0.1484	0.1250	0.0781	0.0625	0.0703
VFScale tr. (ours), hMCTS denoising (energy)	0.6562	0.6094	0.6641	0.7969	0.7969	0.6406	0.4922	0.4922	0.4609	0.4453

Table 11: Success rate of BoN for different training methods on Maze with grid size **15** and Sudoku harder dataset guided with ground truth accuracy. Untrained, BoN (gt) represents use ground truth to guide the BoN. Here,  $L = N$ . Bold font denotes the best model.

Methods	Maze success rate						Sudoku success rate							
	N=1	N=11	N=21	N=41	N=81	N=161	N=1	N=11	N=21	N=41	N=81	N=161	N=321	
Untrained, BoN (gt)	0.0000	0.0000	0.0000	0.0000	0.0000	0.0000	0.0000	0.0000	0.0000	0.0000	0.0000	0.0000	0.0000	
Original, BoN (gt)	0.0625	0.1250	0.1094	0.1328	0.1719	0.1719	0.0859	0.1641	0.2188	0.2344	0.2422	0.2656	0.2969	
DDPM, BoN (gt)	0.0312	0.1094	0.1587	0.1746	0.2031	0.2422	0.0000	0.0000	0.0000	0.0000	0.0000	0.0000	0.0156	
VFScale tr. w/o LRNCL, BoN (gt)	<b>0.2500</b>	<b>0.5078</b>	<b>0.5938</b>	<b>0.6562</b>	<b>0.7109</b>	<b>0.7422</b>	<b>0.1094</b>	<b>0.2578</b>	<b>0.2969</b>	<b>0.3438</b>	<b>0.3750</b>	<b>0.3828</b>	<b>0.4219</b>	

Table 12: Success rate and element-wise accuracy of BoN for different training methods on Sudoku harder dataset guided with ground truth accuracy. Here,  $L = N$ . Bold font denotes the best model.

Methods	Success rate							Element-wise accuracy						
	$N=1$	$N=11$	$N=21$	$N=41$	$N=81$	$N=161$	$N=321$	$N=1$	$N=11$	$N=21$	$N=41$	$N=81$	$N=161$	$N=321$
DDPM, BoN, GT accuracy guided	0.0000	0.0000	0.0000	0.0000	0.0000	0.0000	0.0156	0.5071	0.6089	0.6316	0.6492	0.6691	0.6881	0.6999
Original, BoN, GT accuracy guided	0.0781	0.1641	0.2188	0.2344	0.2422	0.2656	0.2812	<b>0.6650</b>	0.7731	0.7952	0.8036	0.8217	0.8347	0.8491
VFScale tr. w/o LRNCL, BoN, GT accuracy guided	<b>0.1094</b>	<b>0.2578</b>	<b>0.2969</b>	<b>0.3438</b>	<b>0.3750</b>	<b>0.3828</b>	<b>0.4219</b>	0.6442	<b>0.7855</b>	<b>0.8096</b>	<b>0.8317</b>	<b>0.8466</b>	<b>0.8628</b>	<b>0.8854</b>

## E Extension of hMCTS to Conventional Diffusion Models

The inference method hMCTS of VFScale is not limited to energy-based diffusion models. With an external verifier, it can be applied to conventional models that predict noise directly. We validated this on the Maze task by replacing the learned energy with MSE as the reward, confirming hMCTS’s compatibility. Its gains over best-of- $N$  search from the Table 13 below further demonstrate broad applicability across diffusion models.

Table 13: Success rate on Maze (grid size 15) using a conventional noise-predicting diffusion model (DDPM) guided by an external ground-truth verifier. We compare the performance of hMCTS with BoN under different compute budgets ( $N$ ). Here, the reward is defined as the negative MSE to the ground-truth solution. Results validate the compatibility of hMCTS with conventional diffusion and its improved efficiency over best-of- $N$  sampling.

Methods	$N = 1$	$N = 11$	$N = 21$	$N = 41$	$N = 81$	$N = 161$
DDPM, hMCTS, Ground-truth guided	0.0312	0.1328	0.1406	0.1875	0.2188	0.2422
DDPM, BoN, Ground-truth guided	0.0312	0.1094	0.1587	0.1746	0.2031	0.2422

## F Broader Impacts

This paper aims to advance machine learning—particularly diffusion-based generative models. While our improvements promise higher-quality AI-generated content, they also carry potential societal risks. Accordingly, we must remain vigilant to unintended negative outcomes and guard against any unethical or illicit applications of this technology.

## G Limitations and future work

Our inference framework primarily relies on MCTS, which presents two key limitations: (1) limited compatibility with parallel computing, and (2) challenges in effectively evaluating node quality during the early stages of denoising. Future work could explore integrating alternative search strategies, such as those proposed by [28]. Additionally, to enhance performance-energy consistency, we introduce linear-regression negative contrastive learning, which enforces a linear relationship between energy and the distance to real samples. Further investigation is needed to assess the broader implications of this constraint and explore alternative regularization approaches. Lastly, while our current implementation utilizes Gaussian noise for branching, other diffusion-based branching mechanisms remain an open area for exploration.

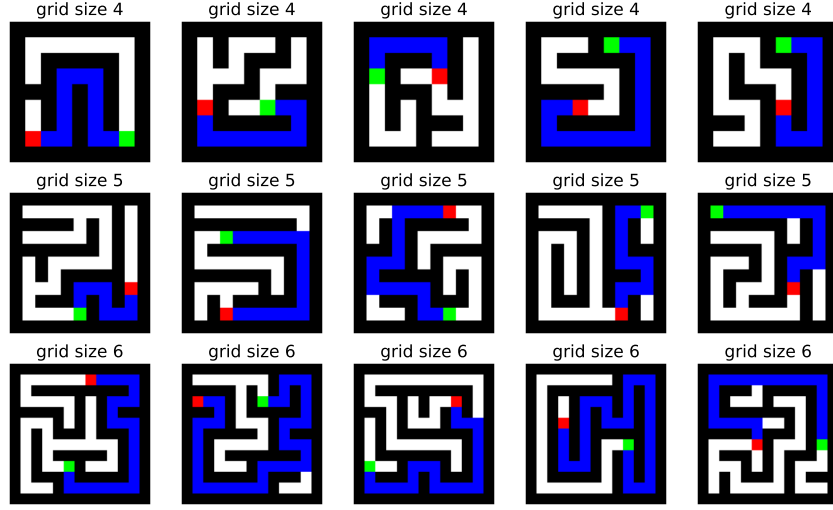


Figure 9: Visualization of training maze dataset.

## H Visualization of results

### H.1 Visualization of Maze experiments

This section presents visualizations of the training in Fig. 9, test Maze data in Fig. 10, and samples generated by different methods in Fig. 11. In the visuals, black pixels denote walls, green represents the starting point, red represents the goal point, blue marks the solved path, and white represents the feasible area. All visualizations are based on a few representative samples. The results from the training and test sets clearly show that the tasks in the test set are notably more challenging than those in the training set. Visual comparisons of samples generated by different methods reveal that the originally trained model, regardless of the inference strategy, performs consistently worse than VFScale.

### H.2 Visualization of Sudoku experiments

This section presents visualizations of the training and test Sudoku data in Fig. 12, and representative samples generated by different methods in Fig. 13. In the visuals, black numbers denote the condition, green numbers represent correct predictions, and red numbers represent wrong predictions. All visualizations are derived from a few representative samples. The comparison between the training and test sets clearly indicates that the tasks in the test set are significantly more difficult than those in the training set. When comparing the samples generated by different methods, it is evident that the originally trained model, regardless of the inference strategy, consistently underperforms compared to VFScale.

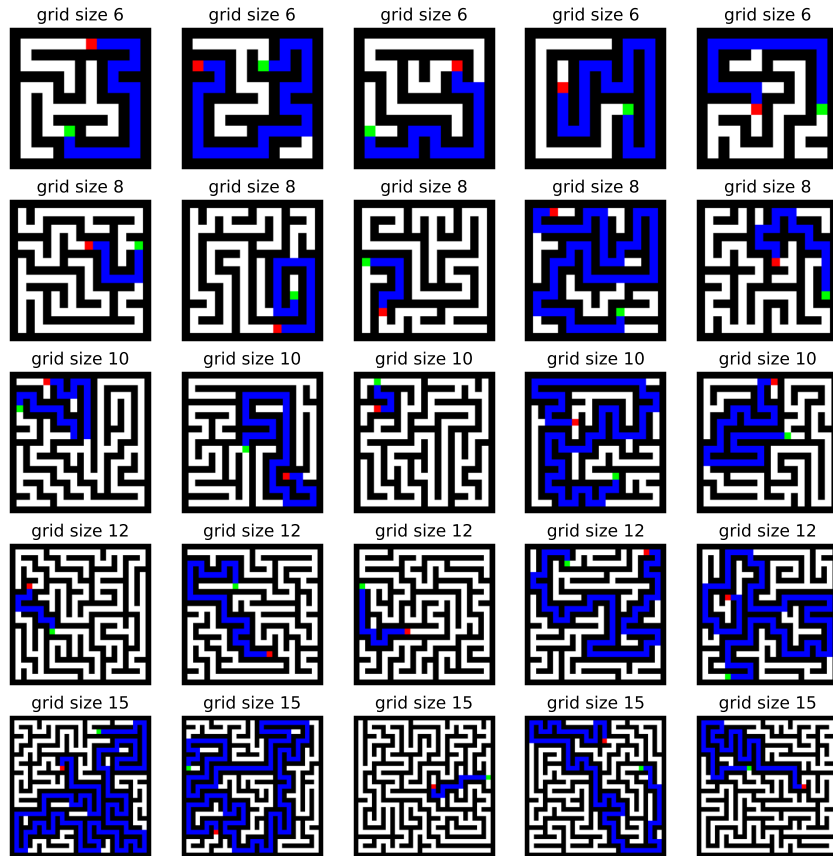


Figure 10: Visualization of test maze dataset, where the blue paths are ground-truth solutions.

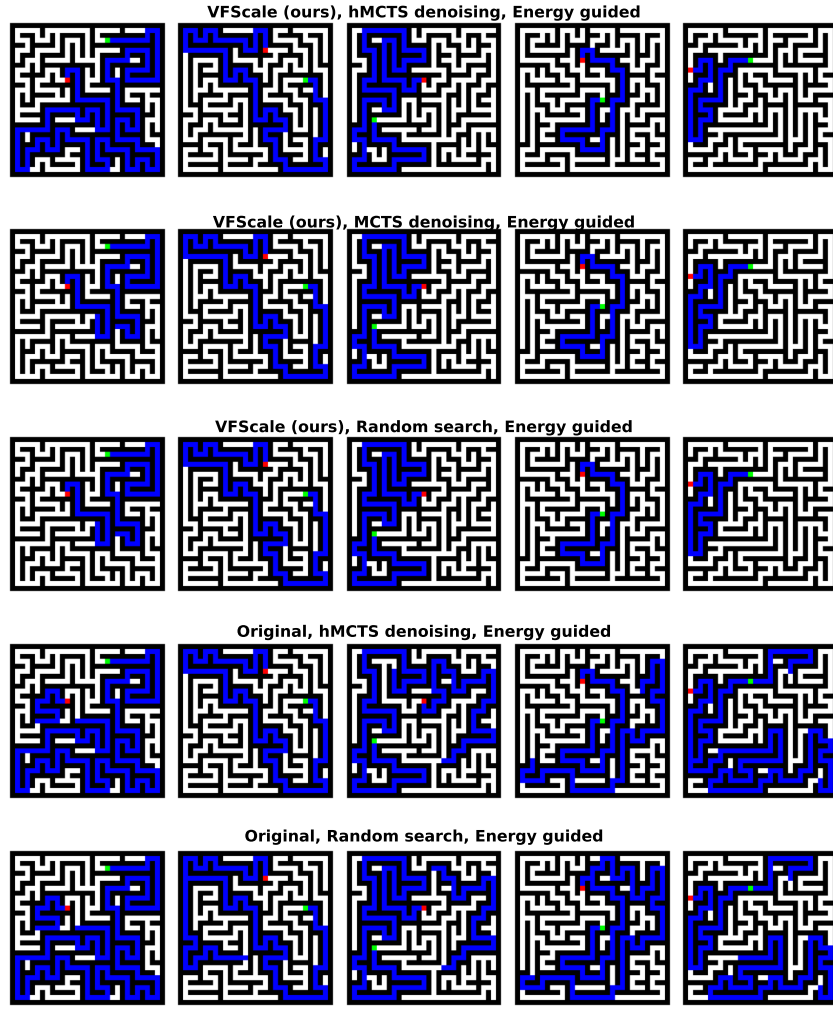


Figure 11: Visualization of samples generated by different training and inference methods.

Train: 32 Entries

9	5							
	3			7	5	6	2	
		1		6	4	3		
	2	7					4	
	4				6	8		
9	5			2	7			
	7	4	3	1	5			
		6		2				
1	3	8	9					

Train: 35 Entries

		3						7
7	9		6	1		2		
	6		8	5			4	
3	7	6						4
1		2	3				8	
	2	7		9	5			
	4	7	2		6	3		
	1			8		9		
		5	1	6			2	

Train: 39 Entries

	8		9		6		2	
2			1	6		7	3	
	5	3	2		4			8
1				4	5	8		9
	7	5						
8	3				9		6	
3	2			7		5		
4	1	9		2	3		6	
		8	4		6		1	

Test: 17 Entries

	2							1
			5		6			
5	6			9				
4							2	
		6				8		
7		2		1				
	3				9			
		8						

Test: 25 Entries

7		1						
		2		7			9	3
						8		
5		6				3		
				6	9			
	2		8		4			
			2	5	3	7		9
2	4	9	6					
						6		

Test: 34 Entries

		6	9		8	7	2	
	5				1			
8	3		1	4			6	
3	7		4			5	8	
			8		1			
9	4	5	3				1	
4			5		3			
2		8			5	1		
9			1		4			

Figure 12: Visualization of training and test Sudoku dataset.

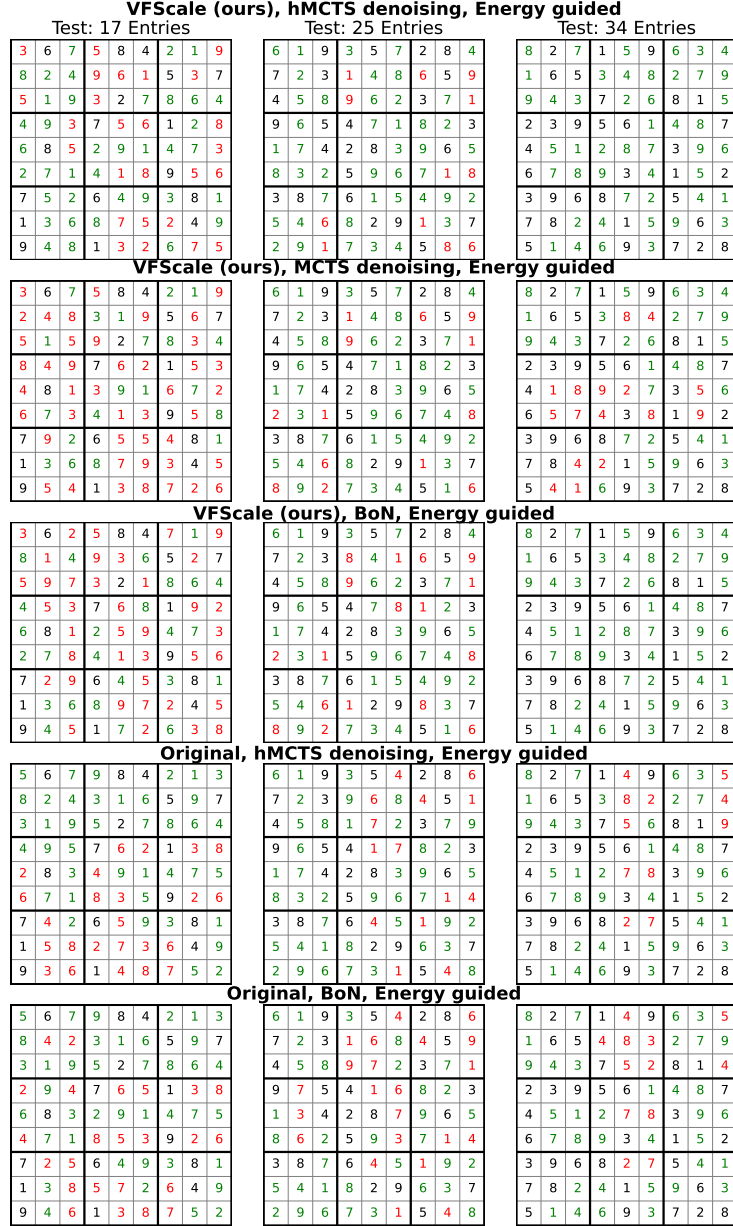


Figure 13: Visualization of samples generated by different training and inference methods.